Article:

Yu, X., Hounslow, M.J. orcid.org/0000-0003-0439-3641 and Reynolds, G.K. (2016) Representing spray zone with cross flow as a well-mixed compartment in a high shear granulator. Powder Technology, 297. pp. 429-437. ISSN 0032-5910

https://doi.org/10.1016/j.powtec.2016.04.053

Representing Spray Zone with Cross Flow as a Well-mixed Compartment in a High Shear Granulator

Xi Yu[1, 2,*], Michael J. Hounslow[2], Gavin K. Reynolds[3]

1 European Bioenergy Research Institute (EBRI), School of Engineering and Applied Science, Aston University, Birmingham B4 7ET, UK
2 Department of Chemical and Biological Engineering, the University of Sheffield, Sheffield, S1 3JD, UK
3 Pharmaceutical Development, AstraZeneca, Macclesfield, SK10 2NA, UK

[*] Corresponding author. Email: x.yu3@aston.ac.uk

Keywords: High shear granulation, Spray zone, Well-mixed compartment

Abstract

The spray zone is an important region to control nucleation of granules in a high shear granulator. In this study, a spray zone with cross flow is quantified as a well-mixed compartment in a high shear granulator. Granulation kinetics are quantitatively derived at both particle-scale and spray zone-scale. Two spatial decay rates, DGSDR (droplet-granule spatial decay rate) ζ_{DG} and DPSDR (droplet-primary particle spatial decay rate) ζ_{DP}, which are functions of volume fraction and diameter of particulate species within the powder bed, are defined to simplify the deduction. It is concluded that in cross flow, explicit analytical results show that the droplet concentration is subject to exponential decay with depth which produces an infinite depth spray zone in a real penetration process. In a well-mixed spray zone, the depth of the spray zone is $4/(\zeta_{DG}+ \zeta_{DP})$ and $\pi^2/3(\zeta_{DG}+ \zeta_{DP})$ in cuboid and cylinder shape, respectively. The first-order droplet-based collision rates of, nucleation rate $B^0$and rewetting rate R_W^0 are uncorrelated with the flow pattern and shape of the spray zone. The second-order droplet-based collision rate, nucleated granule-granule collision rate R_{GG}, is correlated with the mixing pattern. Finally, a real formulation case of a high shear granulation process is used to estimate the size of the spray zone. The results show that the spray zone is a thin layer at the powder bed surface. We present, for the first time, the spray zone as a well-mixed compartment. The granulation kinetics of a

well-mixed spray zone could be integrated into a Population Balance Model (PBM), particularly to aid development of a distributed model for product quality prediction.

1. Introduction

Granulation is a particle production process that allows the design of products by varying the formulation of feeding materials and operating parameters. A series of different types of granulator such as tumbling drum, fluidized bed and high shear granulator are available, and the corresponding operating parameters are optimized to produce granules with desired properties. The research of this area over the last few decades of the 20th Century has been reviewed by Iveson et al [1]. Recent development of granulation technique can be seen (e.g. [2], [3], [4], [5], [6], [7], [8], [9], [10], [11])

The spray zone concept finds application in a wide range of granulators including fluidized bed, high shear mixer or similar devices. The studies of agglomerate formation reveal that product quality can be controlled by changing process parameters which in turn impact critical mechanisms in the spray zone of the fluidized drum granulator [12]. An exploratory surface energy-based spray zone concept has been used to describe surface energy changes of particles traversing the spray zone in a fluidized bed [13]. A novel nucleation apparatus for regime separated granulation was developed to produce narrow sized nuclei from various powder and binder liquid combinations [14]. In this design, the nucleation mechanism is completely separated from all other granulation mechanisms due to the lack of further mechanical mixing of the powder bed, which realizes the idealization of the spray zone as a plug flow reactor. The excellent agreement of agglomerate formation data sets between mixed granulators [15] and ex-granulators [16] demonstrates that the ex-granulator experiments using a spinning riffler under a plug flow field do effectively mirror the spray zone in a mixer granulator.

The spray zone is a special zone with relatively well defined flow field and spatial-preferred transformation kinetics in a granulator. The qualitative definition of the nucleation zone [1] was given to describe the first contact between the powder surface and liquid binder to form the initial nuclei granules which is an important process that dominates in this compartment in the early stages of granulation. Hapgood et al ([16], [17]) demonstrated the critical importance of the nucleation and liquid binder distribution process in determining the size and spread of the final granule size distribution.

All previous literature qualitatively describes the spray zone or develops a micro-scale transformation model to characterize mechanisms occurring in the spray zone. There is no mesoscopic model to link microscopic models and macroscopic models (e.g. Population Balance Model [18], [19]) in describing granulation rates, such as nucleation, in a spray zone. The significance of developing mesoscopic models has been addressed by Michaels [20] in particulate systems. Therefore, in this study, we aim to develop a mesoscopic model of the spray zone in high shear granulator

I. to quantify transformation kinetics and transport phenomena in the spray zone
II. to determine the size of spray zone and estimate volume averaged granulation rates for Population Balance Model
III. to link microscopic models and macroscopic models

1.1. Shape of spray zone

The location of a spray zone is beneath the spraying nozzle and on the surface of powder bed. The nozzle position (height above powder bed) and the spray angle are commonly used to alter the size of the spray zone [1], which means the bed surface area of the spray zone (in x and y coordinates in Fig. 1) is determined by the design and feature of the nozzle. In this study, two geometric shapes (cuboid in Fig. 1a and cylinder Fig. 1b) of the spray zone are considered in the model. In a realistic granulation process, the powder bed will be close to a cross flow arrangement with respect to binder penetration within the spray zone as described in section 2.2.

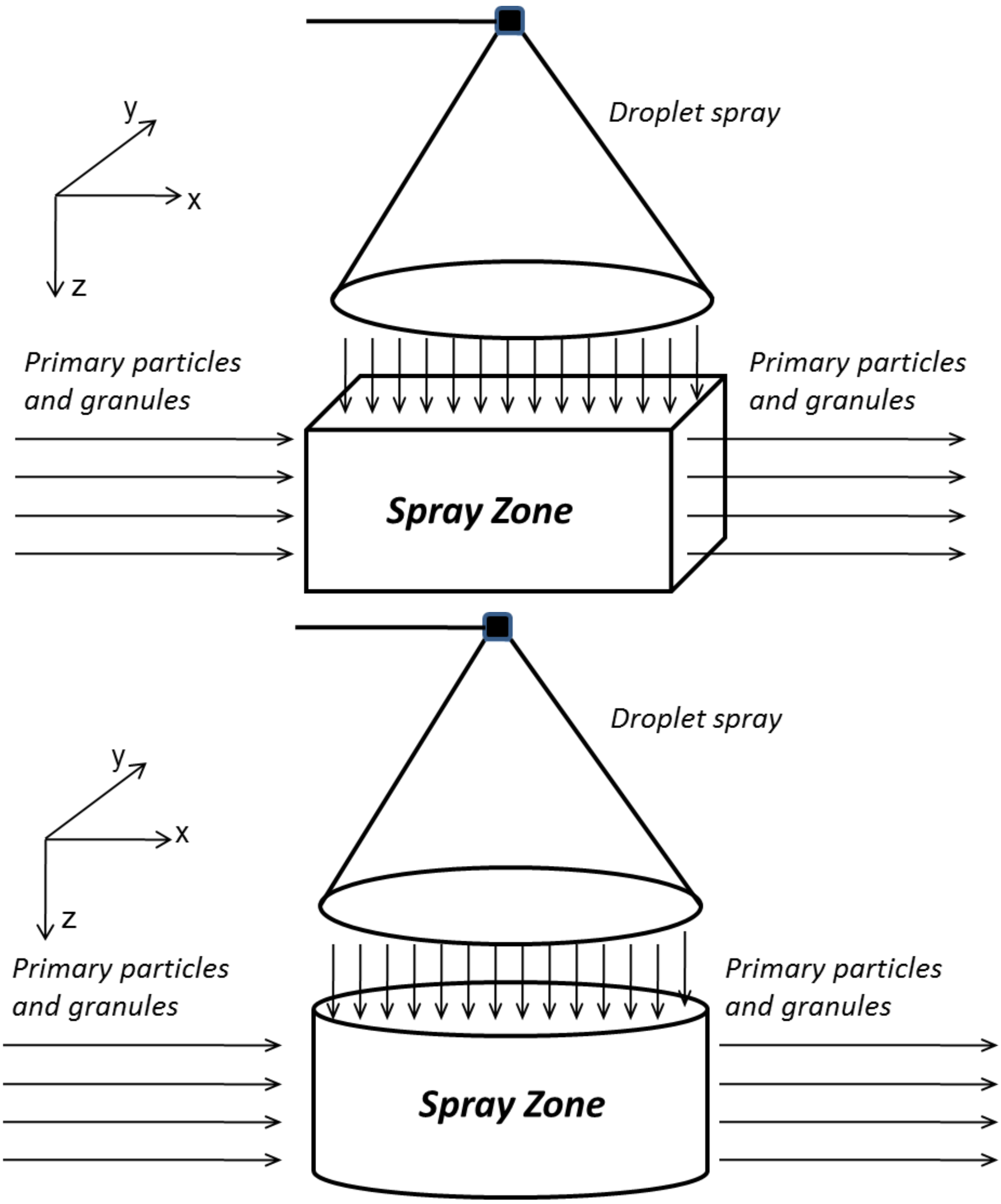

Fig. 1 Schematic of the spray zone with cross flow in a (a) cuboid geometry (b) cylindrical geometry

1.2. Interaction

The interactions among three different particulate species: droplet (liquid binder), primary particle (dry powder) and granule in the spray zone of high shear granulator are addressed in this section. As liquid binder is sprayed on the powder bed surface and penetrates into the powder bed, there are three possible interactions occurring within spray zone including nucleation, rewetting and nucleated granule-granule collision in Fig. 2.

In order to derive analytical solutions of the mathematical model in section 2, reasonable assumptions, based on physical phenomena, are listed as following

(1) Droplet-controlled nucleation [1] occurs in the spray zone. That is to say, one droplet forms a nucleus. Droplet can exist only in the spray zone.

(2) Primary particles are smaller than the droplets in this case. The kinetics of nucleation (Fig. 2) is treated as an immersion mechanism [21].

(3) The rewetting (Fig. 2) occurs when a droplet collides with an existing granule and the droplet is absorbed by the granule.

(4) The collision kernel is based on the binary collision rate of a fast moving droplet (sprayed from the nozzle) collided with a slow moving particle (primary particle or granule).

(5) The deduction is at steady state, and the concentration (number density) of primary particles and existing granules are assumed to be constant.

(6) Nucleated granule-granule collision (Fig. 2): the colliding of two granule nuclei tends to coalesce. Nucleated granule-granule collision rate is treated as a second-order function of droplet concentration. Successful collisions are able to increase the effective nuclei size, which is similar to the coalescence of droplets at the powder bed surface.

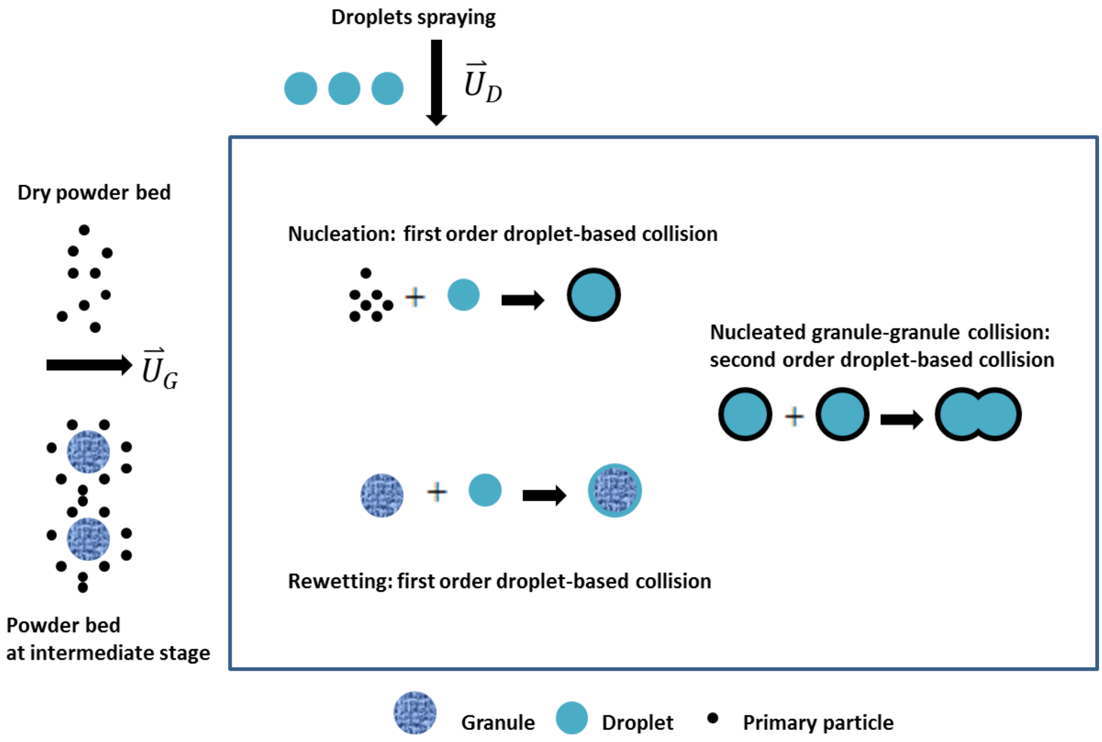

Fig 2 Schematic of three particulate species and their interactions in the spray zone

2. Model

2.1. Mass balance

In this section, a theoretical mathematical model based on the mass balance of droplet (liquid binder), granule and primary particle (dry powder) in the spray zone of high shear granulator is developed.

The mass balance of the droplet, granule and primary particle at steady state respectively are

$$\nabla(\vec{U}_D N_D) + r_{DP} + r_{DG} = 0 \quad (1a)$$

$$\nabla(\vec{U}_G N_G) - r_{DP} = 0 \quad (1b)$$

$$\nabla(\vec{U}_P N_P) - r_{DP}\frac{D_D^2}{D_P^2} = 0 \quad (1c)$$

$\vec{U}_D$ is velocity vector of the droplets, N_D is number density of the droplets, r_{DP}, r_{DG}

are nucleation rate and rewetting rate per unit volume, respectively. Subscripts G, P and D represent granule, primary particle and droplet respectively.

The definition of nucleated granule is: a core droplet with one uniform monolayer of primary particles. So the nucleation rate and rewetting rate are defined as

$$r_{DP} = \beta_{DP} N_P N_D \frac{D_P^2}{D_D^2} \qquad (2a)$$

$$r_{DG} = \beta_{DG} N_G N_D \qquad (2b)$$

β_{DP}, β_{DG} are the collision kernels of the droplet-granule collision and droplet-primary particle collision, respectively. N_G, N_P are the number densities of the granules and primary particles, respectively. D_P, D_D are the diameters of the primary particle and droplet, respectively. The factor D_D^2/D_P^2 is used to describe the "coating" phenomena, giving the number of primary particles covering the surface of one droplet.

Based on the hypothesis (4) in section 1.2, collision kernels of nucleation and rewetting are defined as

$$\beta_{DP} = \frac{\pi}{4} U_D (D_D + D_P)^2 \qquad (3a)$$

$$\beta_{DG} = \frac{\pi}{4} U_D (D_D + D_G)^2 \qquad (3b)$$

D_G is the diameter of the granule

Liquid droplets are assumed to fall vertically on the surface of a powder bed with uniform velocity $\vec{U}_D = (0,0,U_D)$. Then, combining Eq. 2b and 3b to give

$$r_{DG} = \frac{\pi}{4} U_D (D_D + D_G)^2 N_G N_D \qquad (4a)$$

Combining Eq. 2a and 3a to give

$$r_{DP} = \frac{\pi}{4} U_D (D_D + D_P)^2 N_P N_D \frac{D_P^2}{D_D^2} \qquad (4b)$$

Based on a one dimensional constant-velocity assumption of droplet penetration into a powder bed in cross flow, Eq.1 is simplified into a one dimensional equation

$$U_D \frac{dN_D}{dz} + r_{DP} + r_{DG} = 0 \qquad (5)$$

2.2. Cross flow

2.2.1. Cuboid spray zone

Combining Eq. 4a-b and 5 to give N_D as a function of z

$$N_D(z) = N_D(0)e^{-\frac{\pi z\left(D_D^2(D_D+D_G)^2 N_G + D_P^2(D_D+D_P)^2 N_P\right)}{4D_D^2}} \quad (6)$$

$N_D(0)$ is the number density of the droplets at the surface of powder bed, $z = 0$. To simplify Eq. 6, we attempt to replace the number density N by using the volume fraction ε. The voidage of the powder bed ε_A can be measured directly [22] or computed from experimented measurements [23].

Since ε_A is known, the correlations between volume fraction ε, diameter D and number of granules per volume N are

$$\pi D_G^3 N_G/6 = \varepsilon_G \quad (7a)$$

$$\pi D_P^3 N_P/6 = \varepsilon_P \quad (7b)$$

$$\varepsilon_G + \varepsilon_P + \varepsilon_A = 1 \quad (7c)$$

To simplify Eq.6, two new variables DGSDR (droplet-granule spatial decay rate) ζ_{DG} and DPSDR (droplet-primary particle spatial decay rate) ζ_{DP} are defined as

$$(D_D + D_G)^2 \frac{\varepsilon_G}{D_G^3} = \zeta_{DG} \quad (8a)$$

$$(D_D + D_P)^2 \frac{\varepsilon_P}{D_D^2 D_P} = \zeta_{DP} \quad (8b)$$

Combining Eq. 6, 7a-b and 8a-b gives

$$N_D(z) = N_D(0)e^{-\frac{3}{2}z(\zeta_{DG}+\zeta_{DP})} \quad (9)$$

As described in hypothesis (5) in section 1.2, the change of N_G and N_P is negligible at steady state, which is true particularly in the early stage of nucleation in the real granulation process, therefore N_G and N_P are assumed to be constant. Eq. 9 shows that the concentration of droplets is subject to exponential decay, which means $N_D(z)$ decreases at a rate (spatially) proportional to its value:

$$\frac{dN_D}{dz} = -\lambda N_D \quad (10a)$$

$$\lambda = \frac{3}{2}(\zeta_{DG} + \zeta_{DP}) \quad (10b)$$

Where λ is the decay constant. Based on the Eq. 9, it is concluded that the mathematical depth of a spray zone is infinite.

After derivation of N_D(z) in Eq 9, N_G in Eq.1b is examined as below.

As the plug flow of the powder bed is used, Eq.1b is simplified into

$$U_G \frac{dN_G}{dx} - r_{DP} = 0 \tag{11}$$

U_G is moving at the velocity of the powder bed. Combining Eq. 9 and 11 to give

$$N_G(x, z) = N_G(0) + \frac{3x\zeta_{DP} N_D(0) U_D e^{-\frac{3}{2}z(\zeta_{DG}+\zeta_{DP})}}{2U_G} \tag{12}$$

$N_G(0)$ is the number density of the granules located at the boundary where granules are moving in the spray zone, $x = 0$.

The total nucleation rate is the total number of increments per second in the spray zone

$$B^0 = U_G Y \left(\int_0^{+\infty} N_G(X) dz - \int_0^{+\infty} N_G(0) dz \right) = \frac{XYN_D(0)\zeta_{DP} U_D}{(\zeta_{DG} + \zeta_{DP})} \tag{13a}$$

To simplify Eq. 13a, the total feed rate of liquid binder into spray zone is defined as

$$R_D^0 = XYN_D(0)U_D \tag{13b}$$

So Eq. 13a is transformed to

$$B^0 = \frac{\zeta_{DP} R_D^0}{(\zeta_{DG} + \zeta_{DP})} \tag{13c}$$

The total rewetting rate is the total number of droplets consumed by existing granules in spray zone per second

$$R_W^0 = R_D^0 - B^0 = \frac{\zeta_{DG} R_D^0}{(\zeta_{DG} + \zeta_{DP})} \tag{14}$$

The concentration of nucleated granules is the increment of granule concentration in the spray zone from Eq. 12

$$N_G^* = N_G(x) - N_G(0) = \frac{3x\zeta_{DP} N_D(0) U_D e^{-\frac{3}{2}z(\zeta_{DG}+\zeta_{DP})}}{2U_G} \tag{15}$$

Eq 15 shows that N_G^* not only decays exponentially with z, but also increases linearly with x.

If nucleated granule-granule collision occur as hypothesis (6) in section 1.2, even if very small compared with as the second-order rate of droplet concentration, it can be defined as

$$r_{GG} = \beta_{GG} N_G^{*2} \tag{16}$$

The total nucleated granule-granule collision rate in the spray zone is

$$R_{GG} = \int_0^{+\infty} \int_0^{Y} \int_0^{X} r_{GG} dxdydz = -Y\beta_{GG} \frac{a^2 X^3}{6b} \tag{17a}$$

$$a = \frac{3\zeta_{DP} N_D(0) U_D}{2U_G}\ , b = -\frac{3}{2}(\zeta_{DG} + \zeta_{DP}) \tag{17b}$$

Combining Eq.17a and 17b to give

$$R_{GG} = \frac{X\beta_{GG}(\zeta_{DP} R_D^0)^2}{4(\zeta_{DG} + \zeta_{DP}) Y U_G^2} \tag{18}$$

2.2.2. Cylindrical spray zone

The geometry change of the spray zone has no effect on the distribution of droplet concentration along the z direction in Eq. 9. The concentration increment of granules $N_G(x)$ is a function of distance x away from the granule inflow boundary (Eq. 12). The top view of the spray zone in a cylindrical geometry is shown in Fig.3. Point A is an arbitrary spatial position located at the spray zone, x is the distance away from the inlet boundary along powder bed movement, θ is the angle from the positive x axis, R is the radius of the cylinder geometry and r is the distance away from the central axis.

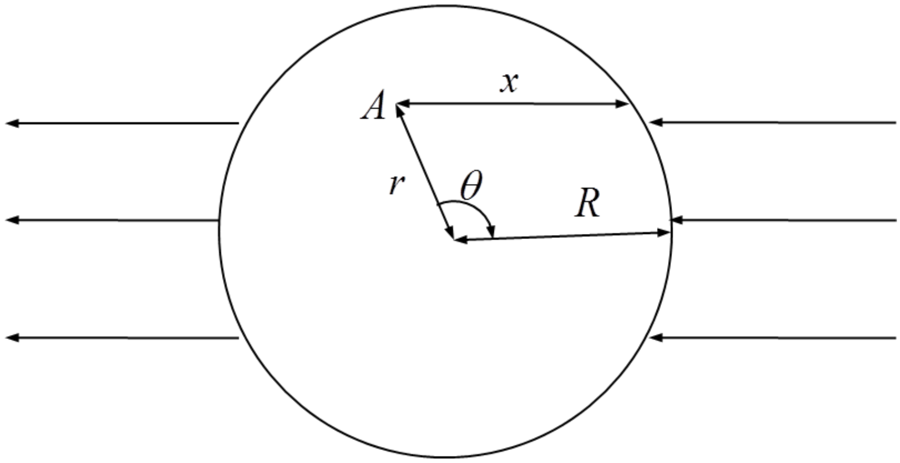

Fig. 3 Top view of the spray zone with cross flow in a cylindrical geometry

x is calculated using triangular relationship

$$x = \sqrt{R^2 - r^2\sin^2\theta} - r\cos\theta \tag{19}$$

when $r = R$ at the boundary of the spray zone

$$x = R(|\cos\theta| - \cos\theta) \tag{20}$$

when $-\frac{\pi}{2} < \theta < \frac{\pi}{2}$ & $r = R$ at the borders of the spray zone where granules are entering, the number density of granules is

$$N_G(\theta) = N_G \tag{21a}$$

When $\frac{\pi}{2} < \theta < \frac{3\pi}{2}$ & $r = R$ at the borders of the spray zone where granules are moving out, the number density of the granules is

$$N_G(\theta) = N_G + \frac{-3R\cos\theta\,\zeta_{DP}N_D(0)U_D e^{-\frac{3}{2}z(\zeta_{DG}+\zeta_{DP})}}{U_G} \tag{22b}$$

The total nucleation rate of the spray zone is

$$B^0 = U_G R\left(\int_{\frac{\pi}{2}}^{\frac{3\pi}{2}}\int_0^{+\infty} -N_G(\theta)\cos\theta dz d\theta - \int_{-\frac{\pi}{2}}^{\frac{\pi}{2}}\int_0^{+\infty} -N_G(\theta)\cos\theta dz d\theta\right)$$

$$= \frac{\zeta_{DP}R_D^0}{(\zeta_{DG} + \zeta_{DP})} \tag{23a}$$

The total rewetting rate of the spray zone is

$$R_W^0 = R_D^0 - B^0 = \frac{\zeta_{DG} R_D^0}{(\zeta_{DG} + \zeta_{DP})} \tag{23b}$$

The total nucleated granule-granule collision of the spray zone is

$$R_{GG} = \int_0^{+\infty} \int_{-\pi/2}^{3\pi/2} \int_0^R r_{GG} r dr d\theta dz = -\beta_{GG} \frac{\pi a^2 R^4}{2b} \tag{24a}$$

$$a = \frac{3\zeta_{DP} N_D(0) U_D}{2U_G}, b = -\frac{3}{2}(\zeta_{DG} + \zeta_{DP}) \tag{24b}$$

Combining Eq. 24a and 24b to obtain

$$R_{GG} = \frac{3\beta_{GG}(\zeta_{DP} R_D^0)^2}{4\pi(\zeta_{DG} + \zeta_{DP}) U_G^2} \tag{25}$$

2.3. Well-mixed flow

2.3.1. Cuboid spray zone

A well-mixed spray zone in a cuboid geometry is shown in Fig 4. The concentration of any species is constant in the well-mixed spray zone.

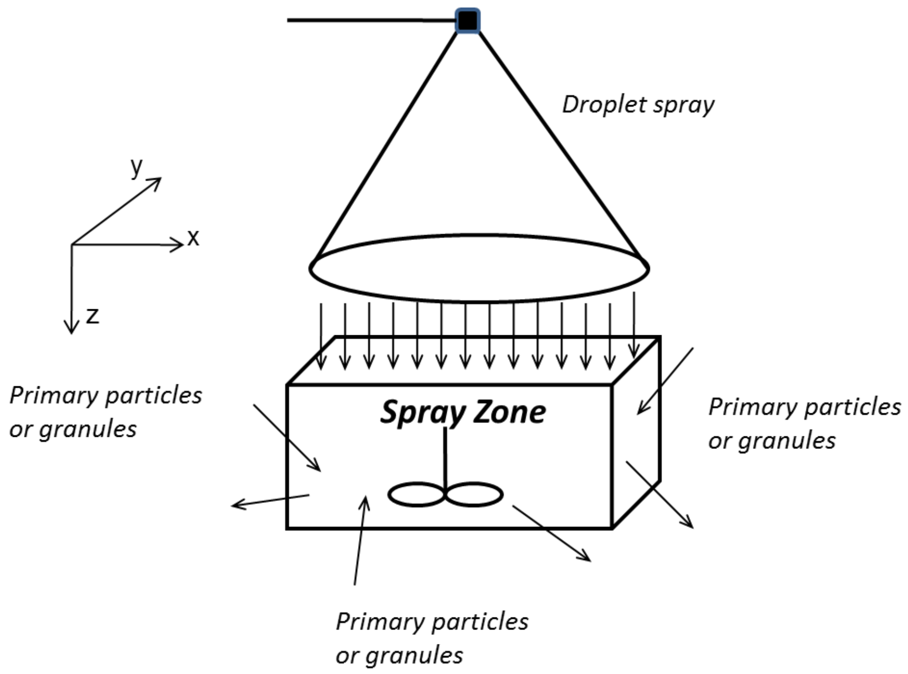

Fig. 4 Schematic of the well mixed spray zone in a cuboid geometry

The mass balance of the droplets is

$$R_D^0 = XYZ(r_{DP} + r_{DG}) \tag{26}$$

Where Z is the depth of the well-mixed spray zone. Combining Eq. 4a-b, 7a-b and 8a-b gives the ratio of r_{DP} to r_{DG}

$$\frac{r_{DP}}{r_{DG}} = \frac{\zeta_{DP}}{\zeta_{DG}} \tag{27}$$

Eq. 27 reveals that the ratio is uncorrelated with the flow pattern (cross flow or well-mixed flow) and does not depend on the size of the spray zone.

Combining Eq. 26 and 27 gives

$$B^0 = XYZr_{DP} = \frac{\zeta_{DP} R_D^0}{\zeta_{DG} + \zeta_{DP}} \tag{28a}$$

$$R_W^0 = XYZr_{DG} = \frac{\zeta_{DG} R_D^0}{\zeta_{DG} + \zeta_{DP}} \tag{28b}$$

By comparing Eq. 13c, 14 and 28a-b, the consistent formulas show that B^0 and R_W^0 are not correlated with the flow pattern (cross flow or well-mixed flow). First-order rates of droplet concentration (nucleation and rewetting rates) are not able to determine the size of well-mixed spray zone.

Combining Eq. 4a-b, 7a-b, 8a-b and 26 gives

$$N_D = \frac{2R_D^0}{3XYZU_D(\zeta_{DG} + \zeta_{DP})} \tag{29}$$

To estimate depth of spray zone Z in Eq. 29, nucleated granule-granule collision is estimated in the well-mixed spray zone.

The mass balance of granules in the spray zone is

$$N_G^* Q = XYZr_{DP} \tag{30}$$

Where Q is volume flow rate of powder bed moving into spray zone, Combining Eq. 28a and 30 gives

$$N_G^* = \frac{\zeta_{DP} R_D^0}{(\zeta_{DG} + \zeta_{DP})Q} \tag{31}$$

Using the definition of r_{GG} in Eq. 16, R_{GG} is

$$R_{GG} = XYZ\beta_{GG}\left(\frac{\zeta_{DP} R_D^0}{(\zeta_{DG} + \zeta_{DP})Q}\right)^2 \tag{32}$$

A well-mixed spray zone with volume XYZ to represent the real spray zone with cross flow requires the same R_{GG} in both flow patterns in Eq. 18 and 32 as below

$$XYZ\beta_{GG}\left(\frac{\zeta_{DP}R_D^0}{(\zeta_{DG}+\zeta_{DP})Q}\right)^2=\frac{X\beta_{GG}(\zeta_{DP}R_D^0)^2}{4(\zeta_{DG}+\zeta_{DP})YU_G^2} \tag{33}$$

Continuing to simplify Eq. 33, the depth of the well-mixed spray zone is

$$Z=\frac{(\zeta_{DG}+\zeta_{DP})Q^2}{4Y^2U_G^2} \tag{34}$$

The flow rate of powder bed at the inlet boundary of the well-mixing spray zone $Q=YZU_G$, then Eq. 34 is transformed into

$$Z=\frac{4}{(\zeta_{DG}+\zeta_{DP})} \tag{35}$$

2.3.2. Cylindrical spray zone

A well-mixed spray zone in a cylindrical geometry is shown in Fig. 5.

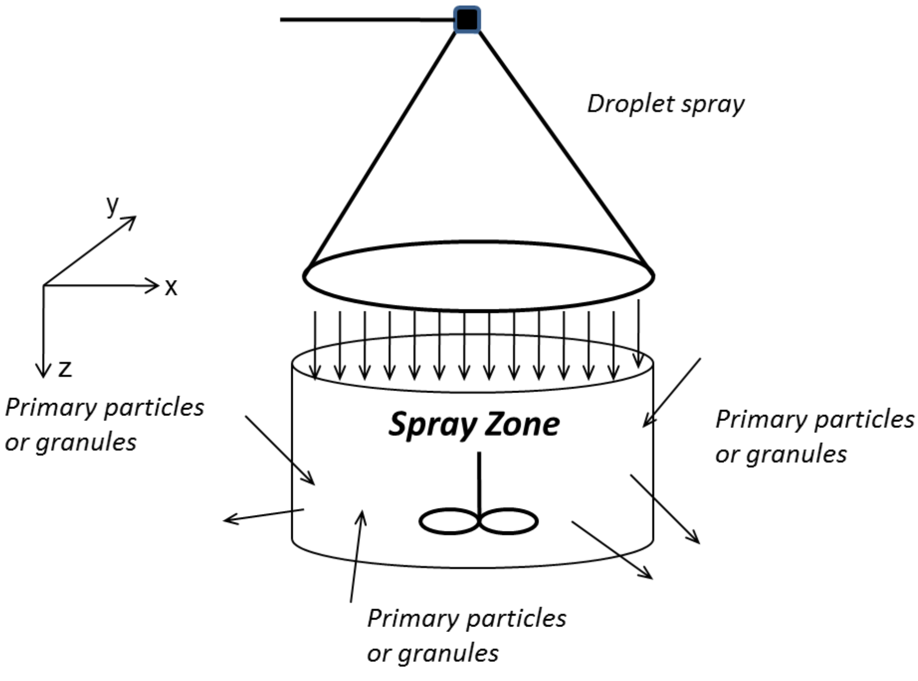

Fig 5 Schematic of the well-mixed spray zone in a cylindrical geometry

The mass balance of the droplets is

$$R_D^0=\pi R^2Z(r_{DP}+r_{DG}) \tag{36}$$

Combining Eq. 27 and 36 gives

$$B^0 = \pi R^2 Z r_{DP} = \frac{\zeta_{DP} R_D^0}{\zeta_{DG} + \zeta_{DP}} \tag{37a}$$

$$R_W^0 = \pi R^2 Z r_{DG} = \frac{\zeta_{DG} R_D^0}{\zeta_{DG} + \zeta_{DP}} \tag{37b}$$

The mass balance of granules in the spray zone is

$$N_G^* Q = \pi R^2 Z r_{DP} \tag{38}$$

Combining Eq. 37a and 38 to give

$$N_G^* = \frac{\zeta_{DP} R_D^0}{(\zeta_{DG} + \zeta_{DP}) Q} \tag{39}$$

Using the definition of $\mathrm{r_{GG}}$ in Eq. 23a, R_{GG} is

$$R_{GG} = \pi R^2 Z \beta_{GG} \left(\frac{\zeta_{DP} R_D^0}{(\zeta_{DG} + \zeta_{DP}) Q} \right)^2 \tag{40}$$

A well-mixed spray zone with volume $\pi R^2 Z$ to represent spray zone with cross flow requires the same R_{GG} in both flow patterns in Eq. 25 and 40 as below

$$\pi R^2 Z \beta_{GG} \left(\frac{\zeta_{DP} R_D^0}{(\zeta_{DG} + \zeta_{DP}) Q} \right)^2 = \frac{3 \beta_{GG} (\zeta_{DP} R_D^0)^2}{4\pi (\zeta_{DG} + \zeta_{DP}) U_G^2} \tag{41}$$

Continuing to simplify Eq. 41, the depth of the well-mixed spray zone is

$$Z = \frac{3 (\zeta_{DG} + \zeta_{DP}) Q^2}{4 \pi^2 R^2 U_G^2} \tag{42}$$

The flow rate of powder bed at the inlet boundary of the well-mixing spray zone $Q = ZRU_G \int_{-\pi/2}^{\pi/2} \cos\theta \, d\theta = 2\, ZRU_G$, then Eq. 42 is transformed into

$$Z = \frac{\pi^2}{3 (\zeta_{DG} + \zeta_{DP})} \tag{43}$$

Comparing penetration depth in Eq. 35 and 43, the constant factor changes from 4 to $\pi^2/3$ by changing the shape of spray zone from cuboid to cylinder.

3. A typical formulation case

Since the formula (Eq. 35 and 43) for the size of a well-mixed spray zone is known, a real granulation case is used as an example to estimate the size of the spray zone.

The mass balance of the powder bed is

$$V\rho_{bulk} = V\frac{\pi D_G^3 \rho_G N_G}{6} + V\frac{\pi D_P^3 \rho_P N_P}{6} + V\varepsilon_A \rho_A \tag{44a}$$

ρ_{bulk} is bulk density of powder bed, V is volume of powder bed

Simplifying Eq. 44a into,

$$\rho_{bulk} = \varepsilon_G \rho_G + \varepsilon_P \rho_P + \varepsilon_A \rho_A \tag{44b}$$

The density of air is negligible relative to that of the powder bed, so $\varepsilon_A \rho_A / \rho_{bulk} \to 0$, and Eq. 44b is changed into

$$\rho_{bulk} = \varepsilon_G \rho_G + \varepsilon_P \rho_P \tag{44c}$$

Before granulation, the bulk density for a dry powder bed is

$$\rho_{bulk} = \varepsilon_P \rho_P \tag{45a}$$

After granulation, the bulk density for a wet powder bed is

$$\rho_{bulk} = \varepsilon_G \rho_G \tag{45b}$$

The bulk density of powder bed and granule (or primary particle) apparent density are able to be measured separately using the method given by Hinkley et al [23]. To roughly estimate the depth of well-mixed spray zone, we give a rational guess on the assumption that the volume fractions of both solid species are the same at the moment of granulation process. The porosity of the powder bed is 0.6. Meanwhile the size data of various species in Table 1 are obtained from a typical formulation case in high shear granulation [24]. The results in Table 1 show that a well-mixed spray zone is a thin layer in depth direction of powder bed.

Table 1 The depth of the spray zone corresponding to particle size and volume fraction

Parameters	D_D (mm)	D_P (mm)	D_G (mm)	ε_G	ε_P	Z (cuboid) (mm)	Z (Cylinder) (mm)
Range	0.05-0.2	0.01-0.1	0.1-2	0.2	0.2		
Typical value	0.1	0.05	1			0.433	0.356
Max value	0.2	0.1	2			0.866	0.712

The depth of spray zone is infinity in cross flow, which unquestionably has no effect on analytical solution, however, in well mixed flow cases, it is not much larger than particle size (e.g. $\boldsymbol{z = 10D_D}$), but it is still right for a continuum analysis, because none of variables is mathematically function of $\boldsymbol{z}$ in well mixed flow. In further application (e.g. PBM) of depth of the spray zone based on the conclusion of this study, the authors recommend suitable adjustment of spray zone to match real granulation process.

4. Conclusion

The spray zone with cross flow is quantified as a well-mixed compartment in a high shear granulator. Granulation kinetics are quantitatively estimated at both particle-scale and spray zone-scale. Two spatial decay rates, DGSDR (ζ_{DG}) and DPSDR (ζ_{DP}), which are functions of volume fraction and diameter of particulate species within the powder bed, are defined to simplify the deduction.

1) In cross flow, explicit analytical results show that the droplet concentration is subject to exponential decay with depth which produces an infinite depth spray zone in a real penetration process.
2) In a well-mixed spray zone, the depths of the spray zones are $4/(\zeta_{\mathrm{DG}}+\zeta_{\mathrm{DP}})$ and $\pi^2/3(\zeta_{\mathrm{DG}}+\zeta_{\mathrm{DP}})$ in cuboid and cylinder shape, respectively.
3) The first-order droplet-based collision rate, nucleation rate B^0 and rewetting R_W^0 are uncorrelated with the flow pattern and shapes of the spray zone.
4) The second-order droplet-based collision rate, nucleated granule-granule collision rate, R_{GG} is correlated with the mixing pattern.
5) A real formulation case for high shear granulation combined with a reasonable estimate of voidages of particulate species within the powder bed is provided to estimate the size of the spray zone. The results show that the spray zone is a thin layer at the powder bed surface.

We present, for the first time, the spray zone as a well-mixed compartment. The granulation kinetics of a well-mixed spray zone could be integrated into PBM, particularly to aid development of a distributed model for product prediction.

Acknowledgment

The authors are grateful to AstraZeneca for funding

Nomenclature

Roman symbols

a	Parameter (m^{-4})
b	Parameter (m^{-1})
B^0	Total nucleation rate (s^{-1})
D	Diameter (m)
N	Number Density (# m^{-3})
Q	Volume flow rate (m^3 s^{-1})
r	Distance away from the central axis (m)
r_{DP}	Nucleation rate per volume unit (m^{-3} s^{-1})
r_{DG}	Rewetting rate per volume unit (m^{-3} s^{-1})
r_{GG}	Collision rate between nucleated granules (m^{-3} s^{-1})
R	Radius of the cylinder geometry (m)
R_D^0	Total feed rate of liquid binder (s^{-1})
R_{GG}	Total collision rate between nucleated granules (m^{-3} s^{-1})
R_W^0	Total rewetting rate (s^{-1})
$\vec{U}$	Velocity vector (m s^{-1})
V	Volume (m^3)
x, X	Length (m)
y, Y	Length (m)
z, Z	Depth (m)

Greek symbols

β	Collision kernel (m^3 s^{-1})
ε	Volume fraction $(-)$
ζ	Spatial decay rate (m^{-1})
θ	Angle from the positive x axis (rad)
λ	Decay constant (m^{-1})
ρ	Density (kg m^{-3})

Subscripts

0 Initial, i.e., at t = 0.

A Air

G Granule

P Primary particle

D Droplet

References

[1] S.M. Iveson, J.D. Litster, K. Hapgood, B.J. Ennis, Nucleation, growth and breakage phenomena in agitated wet granulation processes: a review, Powder Technology, 117 (2001) 3-39.
[2] S. Dale, C. Wassgren, J. Litster, Measuring granule phase volume distributions using X-ray microtomography, Powder Technology, 264 (2014) 550-560.
[3] A.S. El Hagrasy, J.D. Litster, Granulation rate processes in the kneading elements of a twin screw granulator, AIChE Journal, 59 (2013) 4100-4115.
[4] M.X.L. Tan, K.P. Hapgood, Mapping of regimes for the key processes in wet granulation: Foam vs. spray, AIChE Journal, 59 (2013) 2328-2338.
[5] H. Charles-Williams, R. Wengeler, K. Flore, H. Feise, M.J. Hounslow, A.D. Salman, Granulation behaviour of increasingly hydrophobic mixtures, Powder Technology, 238 (2013) 64-76.
[6] C. Mangwandi, M.J. Adams, M.J. Hounslow, A.D. Salman, Influence of fill factor variation in high shear granulation on the post granulation processes: Compression and tablet properties, Powder Technology, 263 (2014) 135-141.
[7] D. Barling, D.A.V. Morton, K. Hapgood, Pharmaceutical dry powder blending and scale-up: Maintaining equivalent mixing conditions using a coloured tracer powder, Powder Technology, 270, Part B (2015) 461-469.
[8] E.L. Chan, K. Washino, H. Ahmadian, A. Bayly, Z. Alam, M.J. Hounslow, A.D. Salman, Dem investigation of horizontal high shear mixer flow behaviour and implications for scale-up, Powder Technology, 270, Part B (2015) 561-568.
[9] T.C. Seem, N.A. Rowson, A. Ingram, Z. Huang, S. Yu, M. de Matas, I. Gabbott, G.K. Reynolds, Twin screw granulation — A literature review, Powder Technology, 276 (2015) 89-102.
[10] S. Oka, H. Emady, O. Kašpar, V. Tokárová, F. Muzzio, F. Štěpánek, R. Ramachandran, The effects of improper mixing and preferential wetting of active and excipient ingredients on content uniformity in high shear wet granulation, Powder Technology, 278 (2015) 266-277.
[11] R. Sayin, A.S. El Hagrasy, J.D. Litster, Distributive mixing elements: Towards improved granule attributes from a twin screw granulation process, Chemical Engineering Science, 125 (2015) 165-175.
[12] J.D. Litster, R. Sarwono, Fluidized drum granulation: studies of agglomerate formation, Powder Technology, 88 (1996) 165-172.
[13] D.K. Kafui, C. Thornton, Fully-3D DEM simulation of fluidised bed spray granulation using an exploratory surface energy-based spray zone concept, Powder Technology, 184 (2008) 177-188.
[14] W.J. Wildeboer, E. Koppendraaier, J.D. Litster, T. Howes, G. Meesters, A novel nucleation apparatus for regime separated granulation, Powder Technology, 171 (2007) 96-105.

[15] J.D. Litster, K.P. Hapgood, J.N. Michaels, A. Sims, M. Roberts, S.K. Kameneni, Scale-up of mixer granulators for effective liquid distribution, Powder Technology, 124 (2002) 272-280.
[16] J.D. Litster, K.P. Hapgood, J.N. Michaels, A. Sims, M. Roberts, S.K. Kameneni, T. Hsu, Liquid distribution in wet granulation: dimensionless spray flux, Powder Technology, 114 (2001) 32-39.
[17] K.P. Hapgood, J.D. Litster, R. Smith, Nucleation regime map for liquid bound granules, AIChE Journal, 49 (2003) 350-361.
[18] X. YU, An in-silico model of granulation, PhD Thesis, Sheffield University, (2012).
[19] X. Yu, M.J. Hounslow, G.K. Reynolds, Accuracy and optimal sampling in Monte Carlo solution of population balance equations, AIChE Journal, 61 (2015) 2394-2402.
[20] J.N. Michaels, Toward rational design of powder processes, Powder Technology, 138 (2003) 1-6.
[21] M.J. Hounslow, M. Oullion, G.K. Reynolds, Kinetic models for granule nucleation by the immersion mechanism, Powder Technology, 189 (2009) 177-189.
[22] M.J. San José, M. Olazar, S. Alvarez, J. Bilbao, Local Bed Voidage in Conical Spouted Beds, Industrial & Engineering Chemistry Research, 37 (1998) 2553-2558.
[23] J. Hinkley, A.G. Waters, D. O'Dea, J.D. Litster, Voidage of ferrous sinter beds: new measurement technique and dependence on feed characteristics, International Journal of Mineral Processing, 41 (1994) 53-69.
[24] M. Oullion, G.K. Reynolds, M.J. Hounslow, Simulating the early stage of high-shear granulation using a two-dimensional Monte-Carlo approach, Chemical Engineering Science, 64 (2009) 673-685.